

## In Vivo Evaluation of Cysteine-Based Chelators for Attachment of $^{99m}\text{Tc}$ to Tumor-Targeting Affibody Molecules

Thuy Tran,<sup>\*,†</sup> Torun Engfeldt,<sup>‡</sup> Anna Orlova,<sup>†,§</sup> Charles Widström,<sup>||</sup> Alexander Bruskin,<sup>⊥</sup> Vladimir Tolmachev,<sup>†,§</sup> and Amelie Eriksson Karlström<sup>‡</sup>

Division of Biomedical Radiation Sciences, Rudbeck Laboratory, Uppsala University, Sweden, School of Biotechnology, Division of Molecular Biotechnology, Royal Institute of Technology, Stockholm, Sweden, Affibody AB, Bromma, Sweden, Hospital Physics, Department of Oncology, Uppsala University Hospital, Uppsala, Sweden, and Russian Research Centrum, Institute of Biophysics, Moscow, Russia. Received September 18, 2006; Revised Manuscript Received January 25, 2007

Affibody molecules present a new class of affinity proteins, which utilizes a scaffold based on a 58-amino acid domain derived from protein A. The small (7 kDa) Affibody molecule can be selected to bind to cell-surface targets with high affinity. An Affibody molecule ( $Z_{\text{HER2:342}}$ ) with a dissociation constant ( $K_d$ ) of 22 pM for binding to the HER2 receptor has been reported earlier. Preclinical and pilot clinical studies have demonstrated the utility of radiolabeled  $Z_{\text{HER2:342}}$  in imaging of HER2-expressing tumors. The small size and cysteine-free structure of Affibody molecules enable complete peptide synthesis and direct incorporation of radionuclide chelators. The goal of this study was to evaluate if incorporation of the natural peptide sequences cysteine-diglycine (CGG) and cysteine-triglycine (CGGG) sequences would enable labeling of Affibody molecules with  $^{99m}\text{Tc}$ . In a model monomeric form, the chelating sequences were incorporated by peptide synthesis. The HER2-binding affinity was 280 and 250 pM for CGG- $Z_{\text{HER2:342}}$  and CGGG- $Z_{\text{HER2:342}}$ , respectively. Conjugates were directly labeled with  $^{99m}\text{Tc}$  with 90% efficiency and preserved the capacity to bind specifically to HER2-expressing cells. The biodistribution in normal mice showed a rapid clearance from the blood and the majority of organs (except kidneys). In the mice bearing SKOV-3 xenografts, tumor uptake of  $^{99m}\text{Tc}$ -CGG- $Z_{\text{HER2:342}}$  was HER2-specific and a tumor-to-blood ratio of 9.2 was obtained at 6 h postinjection. Gamma-camera imaging with  $^{99m}\text{Tc}$ -CGG- $Z_{\text{HER2:342}}$  clearly visualized tumors at 6 h postinjection. The results show that the use of a cysteine-based chelator enables  $^{99m}\text{Tc}$ -labeling of Affibody molecules for imaging.

### INTRODUCTION

In recent years, progress in molecular biology has led to the identification of a number of molecular biomarkers in malignant cells, which can be used as targets for cancer treatment. For example, the elucidation of the role of tyrosine kinase receptors enabled the development of therapy directed to disruption of their signaling (1). Apparently, such therapy can be efficient only if a particular biomarker is present or overexpressed in a particular tumor, i.e., this therapy should be personalized. By now, the major way to determine the presence of a biomarker is a biopsy. However, heterogeneity of biomarker expression causes two problems which may lead to false-negative findings, i.e., sampling errors and discordance in the biomarker expression in primary tumors and metastases (2). The use of radionuclide imaging may help to avoid these problems by imaging both the whole primary tumor volume and the metastases in a single noninvasive procedure.

The use of peptide receptor ligands or their analogues as targeting agents provided excellent clinical results in the detection, e.g., of overexpression of somatostatin receptors (3). This was also a spectacular demonstration of a potential of small, high affinity peptides in radionuclide imaging. However, this approach cannot be applied for imaging of nonreceptor tumor

markers, or for receptors for which no naturally occurring ligands have been identified, such as HER2, which signal by heterodimerization with other receptors (4). For this kind of target, monoclonal antibodies or their Fab or  $F(ab')_2$  fragments were mainly considered as targeting agents. Intact antibody molecules are large glycoproteins (about 150 kDa), which limits their application in molecular imaging. This is due to their relatively slow clearance from the blood circulation, which leads to a high background radioactivity and to their limited extravasation and diffusion into the tumor (5). The use of smaller fragments, e.g.,  $F(ab')_2$ , has enabled high-contrast imaging of tumors (6). The development of even smaller engineered antibody fragments, such as single-chain variable fragments (scFv), has become the mainstream for development of targeting agents for imaging (7). Still, a decrease of the targeting agent size below the size of scFv (approximately 27 kDa) would be appealing. To fulfill this goal, the use of nonimmunoglobulin scaffolds for selection of targeting proteins is promising (8).

Affibody molecules are an example of nonimmunoglobulin scaffolds, which have been successfully applied for *in vivo* imaging. Affibody molecules are based on a 58-amino acid residue protein domain, derived from the B-domain of staphylococcal protein A (9). This low-molecular weight (7 kDa) cysteine-free three-helix bundle protein has become an attractive alternative to antibody-based binding proteins in many applications in biotechnology, separomics, and analysis (see <http://www.affibody.com>). Recently, a new anti-HER2 targeting agent, named Affibody molecule  $Z_{\text{HER2:4}}$ , has been obtained by selection from an affibody library (10). HER2/*neu* (*c-erbB-2*) is a transmembrane receptor tyrosine kinase that mediates the growth, differentiation, and survival of cells (11). Overexpres-

\* Corresponding author. Phone: +46 18 471 3829, fax: +46 18 471 3432, e-mail: thuy.tran@bms.uu.se.

<sup>†</sup> Uppsala University.

<sup>‡</sup> Royal Institute of Technology.

<sup>§</sup> Affibody AB.

<sup>||</sup> Uppsala University Hospital.

<sup>⊥</sup> Russian Research Centrum.

sion of HER2 receptors occurs in 25–30% of human breast and ovarian cancer, and its elevated expression is associated with poor prognosis (12). Herceptin (trastuzumab; Genentech), a humanized monoclonal antibody, is approved for clinical use for treatment of HER2-positive tumors. For the moment, both the American Association of Clinical Oncology and the European Group on Tumor Markers recommend an evaluation of the HER2 status of each breast cancer in order to select patients who will benefit from Herceptin therapy (13, 14). In radionuclide tumor targeting, the radioiodinated (15, 16) and radiobrominated (17) bivalent Affibody ligands ( $Z_{\text{HER2:4}}$ )<sub>2</sub> have been reported to be suitable for visualization of HER2-expressing tumors. Affinity maturation of the  $Z_{\text{HER2:4}}$  Affibody molecule generated a new HER-2 binding clone with a dissociation constant ( $K_d$ ) of 22 pM for binding to the HER2 receptor,  $Z_{\text{HER2:342}}$  (18). This Affibody molecule labeled with iodine or indium radioisotopes showed an excellent *in vivo* visualization of HER2-expressing tumor xenografts (18, 19). The robust cysteine-free structure and the capability to quick refolding enabled synthetic production of Affibody molecules and incorporation of chelators during peptide synthesis.  $Z_{\text{HER2:342}}$  with a DOTA chelator introduced at N-terminal was labeled with <sup>111</sup>In and <sup>68</sup>Ga and was successfully used in a pilot clinical study for imaging of HER2-expression in breast carcinomas (20, 21).

Apparently, the radionuclide technetium-99m would be an attractive label for HER2-targeting Affibody molecules, due to its many favorable features such as low price, high availability, and optimal photon energy (140 keV) for imaging. Besides that, its short half-life ( $T_{1/2} = 6$  h) is a good match to the pharmacokinetics of Affibody molecules, which are characterized by rapid blood clearance. A site-specific technetium labeling of His<sub>6</sub>-( $Z_{\text{HER2:4}}$ )<sub>2</sub> with Tc(I)-carbonyl chemistry was investigated (16). The radiolabeled conjugate provided good tumor accumulation; yet the liver uptake was too high to make it possible to detect liver metastases. For this reason, we started to investigate alternative labeling strategies. Earlier we have evaluated the incorporation of the mercaptoacetyltriglycyl-containing chelating sequence, maGGG (MAG3), for <sup>99m</sup>Tc-labeling of a synthetic variant of  $Z_{\text{HER2:342}}$  (22). This conjugate enables imaging of HER2-expression in LS174T and SKOV-3 xenografts, both at 6 and 24 h pi. However, an appreciable part of the <sup>99m</sup>Tc-maGGG- $Z_{\text{HER2:342}}$  conjugate was excreted via bile, which might complicate the detection of HER2-expression in, e.g., ovarian carcinomas or in extrahepatic abdominal metastases of other tumors at the day of injection.

The strength of the Affibody technology lies in the capacity to generate multimeric constructs and fusion proteins in order to modify affinity/avidity, modulate *in vivo* kinetics, or introduce a peptide/protein effector function. The use of dimerization to increase apparent affinity has been mentioned above. A fusion with an albumin binding domain (ABD) to the dimeric form of  $Z_{\text{HER2:342}}$  was used to prolong residence time in the blood and permit radionuclide therapy using <sup>177</sup>Lu (23). Obviously, such constructs are too large (more than 100 amino acids) to permit peptide synthesis in a cost-efficient way, and recombinant production is therefore required. Although it is possible to couple different chelators to recombinant proteins, this would result in a heterogeneous mixture of conjugates with different modification degree. The use of site-specific labeling would always be preferable, since it provides a more defined targeting agent. It was reported earlier that the introduction of a terminal cysteine in scFv fragments provides a chelating function for <sup>99m</sup>Tc-labeling (24–26). Recent progress in biotechnology, e.g., an introduction of TEV protease (27) which tolerates cysteine at

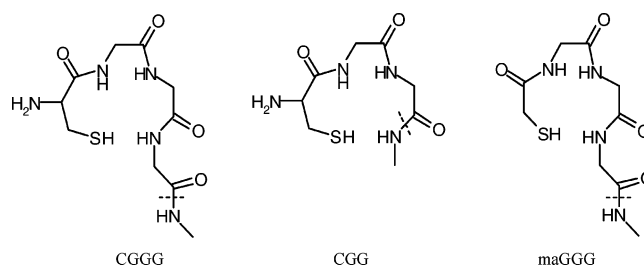


**Figure 1.** Chelator structures.

+1 position of the cleavage site, has also facilitated the recombinant production of proteins with N-terminal cysteine residues.

We hypothesized that the introduction of the <sup>99m</sup>Tc-chelating amino acid sequences cysteine-diglycine (CGG) and cysteine-triglycine (CGGG) (Figure 1) at the N-terminus of Affibody molecules would provide an attachment of <sup>99m</sup>Tc to the Affibody, which is stable enough for an *in vivo* application. The aim of the present study was to evaluate the labeling conditions and the *in vitro* and *in vivo* targeting properties of the <sup>99m</sup>Tc-labeled CGG- and CGGG-containing  $Z_{\text{HER2:342}}$  Affibody conjugates.

## MATERIALS AND METHODS

**Materials.** Fmoc-Ala-OH, Fmoc-Arg(Pbf)-OH, Fmoc-Asn(Trt)-OH, Fmoc-Asp(*t*Bu)-OH, Fmoc-Cys(Trt)-OH, Fmoc-Gln(Trt)-OH, Fmoc-Glu(*t*Bu)-OH, Fmoc-Gly-OH, Fmoc-Ile-OH, Fmoc-Lys(Boc)-OH, Fmoc-Met-OH, Fmoc-Phe-OH, Fmoc-Pro-OH, Fmoc-Ser(*t*Bu)-OH, Fmoc-Trp(Boc)-OH, Fmoc-Tyr(*t*Bu)-OH, and Fmoc-Val-OH were all from Applied Biosystems (Warrington, U.K.). Fmoc-Leu-OH was from Calbiochem-NovaBiochem (Läufelfingen, Switzerland).

*N*-Methylpyrrolidone (NMP) and acetic acid were from VWR. Dichloromethane and acetic anhydride were from Applied Biosystems (Warrington, UK). *N*-Ethyl-diisopropylamine (DIEA) and piperidine were from Lancaster Synthesis (Morecambe, UK). Triisopropylsilane (TIS), trifluoroacetic acid (TFA), and *tert*-butyl methyl ether were from Merck International. Ethanedithiol (EDT) was from Aldrich Chemical Co. Inc. (Milwaukee, WI). 1-Hydroxybenzotriazole (HOBt) and 2-(1*H*-benzotriazol-1-yl)-1,1,3,3-tetramethyluronium hexafluorophosphate (HBTU) were from Advanced ChemTech (Louisville, KY).

For use in comparative biodistribution experiments, the synthetic Affibody molecule maGGG- $Z_{\text{HER2:342}}$  was labeled with <sup>99m</sup>Tc according to a previously published method (22). A recombinant Affibody molecule ( $Z_{\text{HER2:342}}$ ) was indirectly radioiodinated using a succinimidyl ester of *p*-iodobenzoate according to Orlova and co-workers (18) and designated as <sup>125</sup>I-PIB- $Z_{\text{HER2:342}}$ . An Ultra-TechneKow generator from Tyco was eluted with sterile 0.9% sodium chloride (Mallinckrodt Medical BV, Petten, The Netherlands) to obtain <sup>99m</sup>Tc as pertechnetate.

**Instrumentation.** An automated gamma-counter with a 3 in. NaI(Tl) detector (1480 Wizard, Wallac Oy, Turku, Finland) was used to measure the radioactivity. An instant thin layer chromatography analysis was performed using silica gel impregnated glass fiber sheets, ITLC strips (ITLC SG, from Gelman Sciences Inc). The Cyclone Storage Phosphor System and the OptiQuant image analysis software (both from Packard) were used to measure the radioactivity on the ITLC strips. The cells were counted in an electronic cell counter (Beckman Coulter, Fullerton, CA). *In vivo* imaging was performed by a dual-head e. Cam gamma camera (Siemens Medical Systems, Inc.), equipped with a low-energy, high-resolution collimator (LEHR). The acquisition of static images was performed with a 256 × 256 matrix and a zoom factor of 3.2. The energy window settings were 140 keV, 15%.

**Peptide Synthesis.** Z<sub>HER2:342</sub> was synthesized using Fmoc-chemistry on a 433A Peptide Synthesizer (Applied Biosystems, Warrington, U.K.) as previously described (25). Ten molar equivalents of amino acid were activated with HBTU and HOBt in NMP for each coupling reaction. Fmoc deprotection was performed by treatment with 20% piperidine–NMP. A double coupling procedure was used at 17 selected positions to increase the synthetic yield, and acetic anhydride was used to cap any remaining free amino groups. The peptide sequence is VENKFNKEMRNAYWEIALLPNLNNQQKRAFIRSLYDDPSQSANLLAEAKKLNDQAQPK, with double coupled amino acids underlined.

After the automatic assembly of Z<sub>HER2:342</sub>, the N-terminal of the peptide was manually extended with the Tc-chelating sequences CGG and CGGG by coupling each amino acid with 5 mol equiv of amino acid, HBTU, and HOBt and 10 equiv of DIEA in NMP for 20 min. 20% piperidine–NMP was used for removal of the N-terminal Fmoc protecting group. Kaiser tests were performed to evaluate if the acylation and deprotection reactions were successful or had to be repeated. The manual coupling step of the chelators was used, since it is a rapid and easy way to introduce different chelating amino acid residues.

The resin-bound peptide was incubated with TFA/EDT/TIS/H<sub>2</sub>O (94:2.5:2.5:1) for 2 h to remove permanent protecting groups and liberate the peptide from the solid support. The peptide was extracted in *tert*-butyl methyl ether–H<sub>2</sub>O (50:50), filtered, and lyophilized. The crude synthetic product was analyzed by analytical RP-HPLC using a 4.6 × 150 mm polystyrene/divinylbenzene matrix column with a particle size of 5 μm (Amersham Biosciences, Uppsala, Sweden), a 20 min gradient of 20–60% B (A: 0.1% TFA–H<sub>2</sub>O, B: 0.1% TFA–CH<sub>3</sub>CN) and a flow rate of 1 mL/min. All peptides were purified using a 20 min gradient of 25–45% B. The pure product was lyophilized, and the final peptide concentration was determined by amino acid analysis (Aminosyraanalyscentralen, Uppsala, Sweden). To verify the identity of the peptides, the peptide mass was analyzed on a Q-ToF II mass spectrometer fitted with an ESI source (Waters Corporation, Micromass MS Technologies, Manchester, U.K.). The Maximum Entropy 1 (MaxEnt1) algorithm was used to deconvolute the isotopic and charge state information. For the labeling experiments, the freeze-dried peptides were dissolved in degassed, deionized water to a concentration of 1 mg/mL and were stored at –20 °C.

**Biophysical Characterization.** The melting point of each peptide was determined on a Jasco J-810 spectropolarimeter (JASCO, Tokyo, Japan). The temperature was increased from 20 to 90 °C at a rate of 5 °C/min, and the absorbance was detected at 221 nm. In addition, CD spectra were recorded from 250 to 195 nm at 20 °C before and after melting. The sample concentration was 50 μM in PBS pH 7.4 and the optical path length was 1 mm.

**Biosensor Analysis.** The binding kinetics of the different peptides were compared by performing a real-time biospecific interaction analysis on a Biacore 2000 instrument (Biacore, Uppsala, Sweden). HBS (10 mM HEPES, 150 mM NaCl, 3.4 mM EDTA, 0.005% Surfactant P20, pH 7.4) was used as running buffer at a flow rate of 50 μL/min, and also for dilution of the samples into the concentration range 0.3–10 nM. 500 RU (response units) of recombinant extracellular domain of HER2 (a generous gift from Prof. Gregory Adams, Fox Chase Cancer Center, Philadelphia, PA) and 900 RU of human serum albumin, HSA (KabiVitrum, Stockholm, Sweden), were immobilized onto a CM5 sensor chip (Biacore, Uppsala, Sweden) from 20 μg/mL solutions in 10 mM NaAc pH 4.5. The association time was 5 min, and the dissociation time was 10 min, followed by regeneration with 20 μL of 20 mM HCl. The

BiaEval software (Biacore, Uppsala, Sweden) and the Langmuir 1:1 binding model were used for the kinetic analysis.

**Labeling with <sup>99m</sup>Tc.** The analysis of the labeled Affibody molecules was done by ITLC. To determine labeling yield and stability, ITLC strips were eluted with PBS. Validation experiments showed that pertechnetate, as well as tartrate, glucoheptonate, and cysteine complexes of <sup>99m</sup>Tc migrated with the eluent front, while the Affibody remained at the origin in PBS. To determine the presence of reduced hydrolyzed technetium, ITLC was eluted with pyridine:acetic acid:water (5:3:1.5). In this eluent, the technetium colloids remained at the origin, while the radiolabeled Affibody, pertechnetate, and tartrate complexes of <sup>99m</sup>Tc migrated with solvent front.

Two variants of labeling procedures were evaluated.

**Indirect labeling** of CGGG-Z<sub>HER2:342</sub> was performed according to Winnard et al. (29). CGGG-Z<sub>HER2:342</sub> (20 μL, 1 mg/mL in deionized degassed water) was mixed with 80 μL of PBS and 20 μL of a solution containing Na/K tartrate in 0.5 M NaHCO<sub>3</sub> and 0.25 M NH<sub>4</sub>OAc. If necessary, 0.15 M NaOH was added to keep the pH of the final mixture at about 11. A fresh <sup>99m</sup>Tc-generator eluate (50–350 μL) followed by SnCl<sub>2</sub>·2H<sub>2</sub>O in 0.01 M HCl (10 μL, 1 mg/mL) was added, and the mixture was incubated at room temperature for 60 min.

**Direct labeling:** 20 μL of CGG-Z<sub>HER2:342</sub> or CGGG-Z<sub>HER2:342</sub> (1 mg/mL in deionized degassed water) was mixed with 20 μL of 0.15 M NaOH to obtain a final pH of about 11. A solution of SnCl<sub>2</sub>·2H<sub>2</sub>O in 0.01 M HCl (10 μL, 1 mg/mL) was added to the mixture, followed by 100–200 μL of fresh pertechnetate solution. The mixture was slightly vortexed and incubated at room temperature for 60 min.

After being labeled, <sup>99m</sup>Tc-CGG-Z<sub>HER2:342</sub> and <sup>99m</sup>Tc-CGGG-Z<sub>HER2:342</sub> were isolated from unreacted technetium and other low-molecular weight components using size-exclusion chromatography on disposable NAP-5 columns (Amersham Pharmacia Biotech AB, Uppsala, Sweden) preequilibrated with PBS. The purity of the final product was assessed by analysis with ITLC.

**Stability Test.** The stability of the labeled Affibody conjugates was tested in PBS and in 300 molar excess of cysteine. After purification, 100 μL of labeled conjugates was added to 500 μL of PBS. The solutions were stored at room temperature for 2 h and were analyzed using ITLC. In the cysteine challenge test, a fresh solution of cysteine was prepared (1 mg/mL in PBS, pH 7.0). The radiolabeled conjugates were added to a final molar ratio of cysteine to peptide of 300:1. The test tubes were incubated for 2 h at 37 °C, and the radiochemical purity was analyzed using ITLC. All experiments were performed in triplicate.

To analyze the serum stability, blood was collected from NMRI mice using a heparinized syringe. The blood was centrifuged at 5000g, and serum was collected, divided into 0.5 mL aliquots, and stored frozen before use. Serum samples were unfrozen immediately before the stability test. The test was performed in triplicate. The serum samples (240 μL) were mixed with freshly labeled <sup>99m</sup>Tc-CGG- and <sup>99m</sup>Tc-CGGG-Z<sub>HER2:342</sub> (10 μL) to obtain an Affibody molecule concentration similar to their concentration in blood at the moment of injection. The samples were incubated for 1 h at 37 °C. After incubation, the tested samples were analyzed by SDS-PAGE on NuPAGE 4–12% Bis-Tris Gel (Invitrogen) in MES buffer (200 V constant, 35 min). To facilitate interpretation of the result, a sample of <sup>99m</sup>Tc-pertechnetate was run in parallel with the test sample on the same gel. After the analysis, the gels were dried, and radioactivity distribution along the gels was evaluated using Cyclone Storage Phosphor System.

**Cell Culture.** The HER2-expressing ovarian carcinoma cell line SKOV-3, displaying approximately 1.2 × 10<sup>6</sup> HER2

**Table 1. Peptide Synthesis and Characterization Data**

peptide	synthetic yield (%)	theoret mw (Da)	exptl mw (Da)	$K_D$ (pM)	$T_m$ (°C)
Z <sub>HER2:342</sub>	21	6718	6718	80	64
CGG-Z <sub>HER2:342</sub>	16	6993	6992	280	68
CGGG-Z <sub>HER2:342</sub>	16	7050	7050	250	68

**Table 2. Labeling and *in Vitro* Characterization of Radiolabeled Conjugates**

	<sup>99m</sup> Tc-CGGG-Z <sub>HER2:342</sub>		<sup>99m</sup> Tc-CGG-Z <sub>HER2:342</sub>
	indirect	direct	direct
labeling yield, %	53.8 ± 10.1	90.4 ± 3.9	94.1 ± 2.6
isolated yield, %	49.3 ± 9.1	72.4 ± 5.8	69.0 ± 4.0
purity, %	98.0 ± 1.5	98.1 ± 2.0	99.0 ± 1.0
antigen binding capacity	75.0 ± 11.6	62.5 ± 13.4	57.1 ± 1.7
stability during cysteine challenge	66.9 ± 14.6	69.6 ± 6.2	70.8 ± 6.3
PBS stability	85.0 ± 17.0	82.7 ± 4.6	90.6 ± 4.6

receptors per cell, was used in this study. The cell line was cultured in McCoy's medium (Flow Irvine, UK), supplemented with 10% fetal calf serum (Sigma), 2 mM L-glutamine, and PEST (penicillin 100 U/mL and 100 μg/mL streptomycin), all from Biokrom Kg, Germany. The cells were cultured at 37 °C in a humidified incubator with 5% CO<sub>2</sub> and trypsinized using trypsin-EDTA solution (0.25% trypsin, 0.02% EDTA, Biokrom Kg, Germany). The SKOV-3 cells were cultivated on Petri dishes with a diameter of 3.5 cm to a cell density of 2 to 5 × 10<sup>5</sup> cells per dish.

**Binding Specificity of <sup>99m</sup>Tc-Labeled Conjugates to HER2-Expressing Cells.** Labeled conjugates were added to two groups of Petri dishes (three dishes per group) with a calculated ratio of one labeled Affibody conjugate per one HER2 receptor. One group of dishes was presaturated with a 100-fold excess of nonlabeled Affibody 10 min before the labeled conjugate was added. Cells were incubated for 1 h at 37 °C, and the incubation media was collected. The cell dishes were washed six times with cold serum-free medium and treated with 0.5 mL trypsin-EDTA for 10 min at 37 °C. When the cells were detached, 0.5 mL complete medium was added to each dish and the cells were resuspended. The cell suspension was used for radioactivity measurements.

**Cellular Retention after Interrupted Incubation with <sup>99m</sup>Tc-Labeled Z<sub>HER2:342</sub>.** Labeled conjugate, 0.8 ng/10<sup>5</sup> cells, was added in 1 mL of complete medium to a series of Petri dishes containing SKOV-3 cells. The dishes were incubated for 2 h at 37 °C, and the incubation medium was removed. The cells were washed six times with ice-cold serum-free medium, and after addition of 1 mL of complete medium, the cell dishes were incubated further at 37 °C. At designated times of incubation (0.5, 1, 2, 4, 8, and 24 h), a group of three dishes was analyzed for cell-associated radioactivity. The media were collected in scintillation tubes, and the cells were washed six times with ice-cold serum-free medium and treated with 0.5 mL of trypsin-EDTA solution for 10 min at 37 °C. After addition of 0.5 mL of complete medium, the cells were resuspended and collected in scintillation tubes. The radioactivity content of the samples was measured on an automated gamma-counter.

**Antigen Binding Capacity.** The SKOV-3 cells were scraped from the surface in order to preserve the receptor expression. After resuspension of scraped cells in medium, the cells were counted in an automated cell counter, and cell pellets containing 6 × 10<sup>6</sup> cells were formed in Eppendorf tubes by gentle centrifugation (2 min at 2500g). The analysis was done in triplicate. The supernatant was removed completely, and 1 mL of medium with labeled conjugate (with a ratio of approximately one Affibody molecule per 100 HER2 receptors) was added.

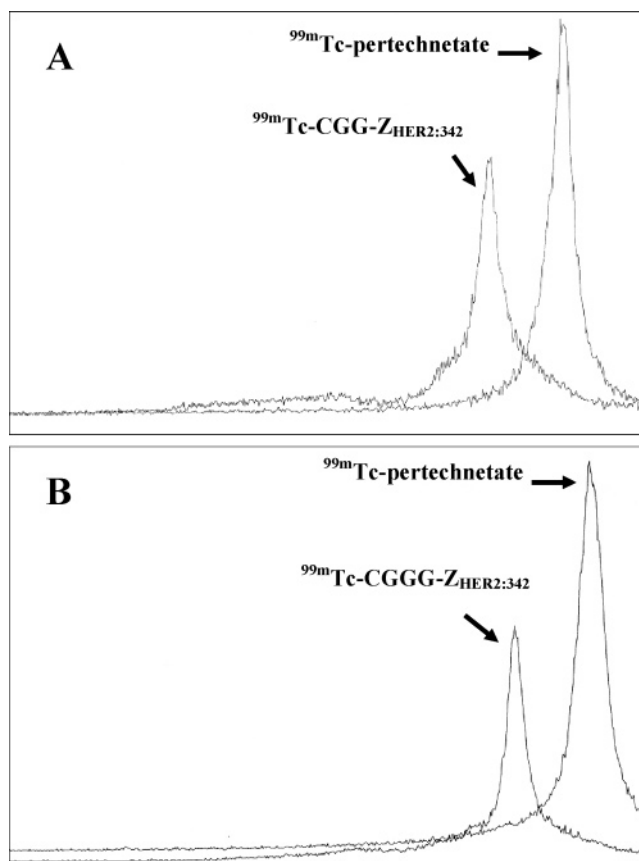


**Figure 2.** Analysis of <sup>99m</sup>Tc-CGG-Z<sub>HER2:342</sub> (A) and <sup>99m</sup>Tc-CGGG-Z<sub>HER2:342</sub> (B) stability in serum. A sample of each conjugate was incubated in blood serum for 1 h at 37 °C and analyzed using SDS PAGE and radioactivity distribution on the gel was measured using a PhosphorImager.

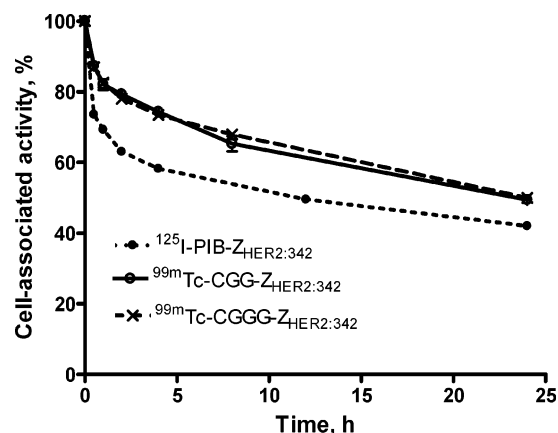


**Figure 3.** Cell-associated radioactivity as a function of time after interrupted incubation of SKOV-3 cells with radiolabeled Z<sub>HER2:342</sub>. The cell-associated radioactivity at time zero after the interrupted incubation was considered as 100%. Data are presented as mean ± SD ( $n = 3$ ). Error bars might not be seen, because they are smaller than point symbols.

The cells were gently resuspended and incubated for 4 h at 4 °C under slight shaking. After incubation, the cells were centrifuged (8 min at 7500g), and 0.5 mL supernatant medium was taken to a separate Eppendorf tube. The radioactivity was measured on both samples, and the antigen binding capacity (ABC) was calculated as  $ABC = (A - B)/(A + B) \times 100\%$ , where  $A$  is the radioactivity of the Eppendorf tube containing both the cell pellet and 0.5 mL supernatant, and  $B$  is the radioactivity of the Eppendorf tube containing 0.5 mL supernatant only.

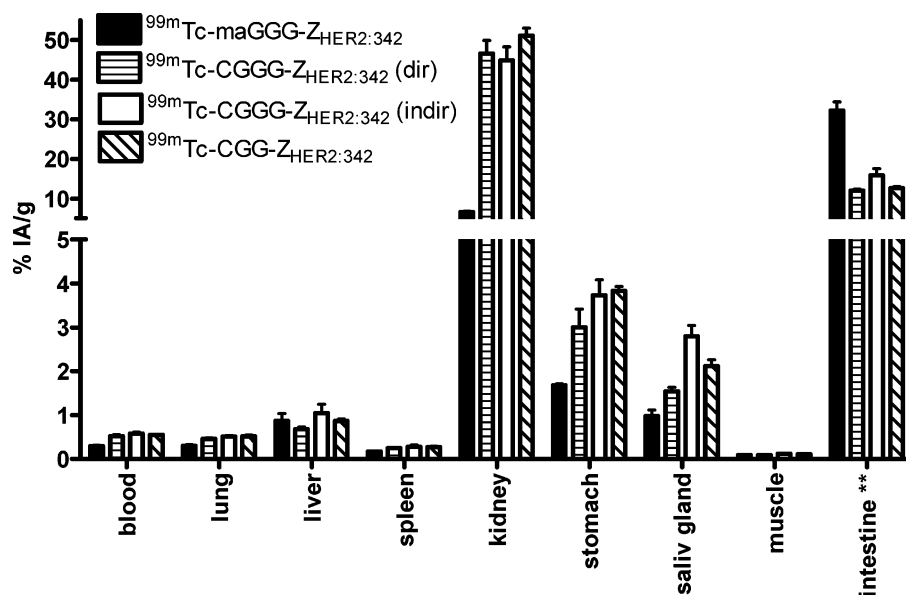


**Figure 4.** Biodistribution of radiolabeled Affibody molecules in NMRI normal mice 4 h pi. Data are presented as an average from four animals  $\pm$  SEM.  $^{99m}\text{Tc}$ -maGGG- $\text{Z}_{\text{HER}2:342}$  was included in the experiment for comparison. Uptake in spleen and muscle was less than 0.3% IA/g.

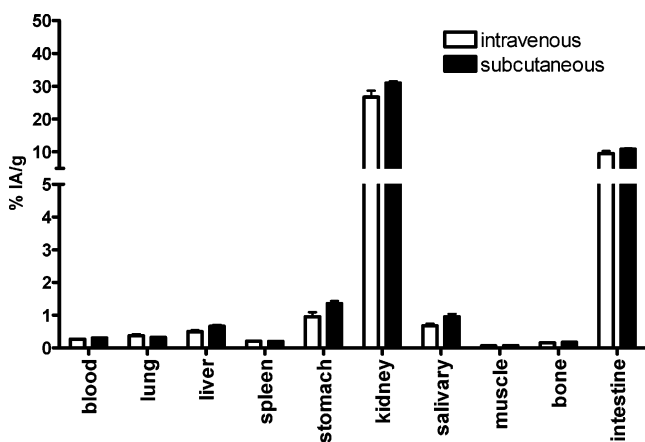


**Figure 5.** Biodistribution of  $^{99m}\text{Tc}$ -CGG- $\text{Z}_{\text{HER}2:342}$  in NMRI mice after intravenous and subcutaneous injection (4 h pi). Data are presented as an average from four animals  $\pm$  SEM.

**Animal Model.** The animal study was approved by the Local Ethics Committee for Animal Research. In comparative biodistribution studies, non-tumor-bearing NMRI mice were used. In tumor targeting and imaging experiments using  $^{99m}\text{Tc}$ -CGG- $\text{Z}_{\text{HER}2:342}$ , female Balb/c nu/nu mice were used. The animals (10–12 weeks old at arrival) were acclimatized for one week at the Rudbeck laboratory animal facility using standard diet, bedding, and environment before tumor implantation. The tumor was grafted by subcutaneous (sc) injection of  $\sim 10^7$  SKOV-3 cells in the right hind leg. Xenografts were allowed to develop during 2 months.

In all biodistribution studies, the mice were euthanized at predetermined time points with an intraperitoneal injection of Ketalar-Rompun solution (20  $\mu\text{L}$  of solution per gram of body weight: Ketalar [ketamine], 10 mg/mL; Rompun [xylazine], 1 mg/mL). The mice were punctured in the heart with a 1 mL syringe rinsed with diluted heparin (5000 IE/mL, from Leo Pharma, Copenhagen, Denmark). Blood and organ samples were taken and weighed, and their radioactivity was recorded using an automatic gamma-counter with standard  $^{99m}\text{Tc}$  protocol. The background was measured for each sample holder in the same way. The tissue uptake values were calculated as percent injected activity per gram tissue (% IA/g).

**Comparative Biodistributions in Non-Tumor-Bearing NMRI Mice.** Sixteen mice were randomly divided into four

groups with four animals each. Each group of mice was injected subcutaneously with 1  $\mu\text{g}$  ( $\sim 100$  kBq in 100  $\mu\text{L}$  of PBS) of  $^{99m}\text{Tc}$ -CGG- $\text{Z}_{\text{HER}2:342}$ ,  $^{99m}\text{Tc}$ -CGGG- $\text{Z}_{\text{HER}2:342}$  (directly labeled),  $^{99m}\text{Tc}$ -CGGG- $\text{Z}_{\text{HER}2:342}$  (indirectly labeled), or  $^{99m}\text{Tc}$ -maGGG- $\text{Z}_{\text{HER}2:342}$ , respectively. After 4 h, the mice were euthanized, and samples of blood, lung, liver, kidney, stomach, salivary glands, spleen, muscle, and intestines were collected.

In a separate study, two groups of four animals each were injected with the same batch of  $^{99m}\text{Tc}$ -CGG- $\text{Z}_{\text{HER}2:342}$ , but one group was injected intravenously and another subcutaneously. After 4 h, the mice were euthanized and the biodistribution of radioactivity was performed as described above.

**Tumor Targeting in Balb/c nu/nu Mice with SKOV-3 Xenografts.** Sixteen mice were randomly divided into four groups with four animals each. One group of mice was injected subcutaneously with 0.5 mg of nonlabeled recombinant  $\text{Z}_{\text{HER}2:342}$  in 250  $\mu\text{L}$  of PBS 1 h before radioactive injection. All mice were sc co-injected with  $^{99m}\text{Tc}$ -CGG- $\text{Z}_{\text{HER}2:342}$  and  $^{125}\text{I}$ -PIB- $\text{Z}_{\text{HER}2:342}$  (totally 1  $\mu\text{g}$  Affibody ligand, totally  $\sim 100$  kBq in 100  $\mu\text{L}$  of PBS). After 1, 4, and 6 h pi, respectively, the mice were euthanized as described earlier. The mice in the blocking group were euthanized 4 h pi. Organ and tissue samples were taken, and their radioactivity uptake was determined as percent injected activity per gram tissue (%IA/g).

**Gamma-Camera Imaging of HER2-Expressing Xenografts Using  $^{99m}\text{Tc}$ -CGG- $\text{Z}_{\text{HER}2:342}$ .** Experimental tumor imaging was performed in two mice bearing SKOV-3 xenografts. The animals were intravenously injected through the tail with 3 MBq (10  $\mu\text{g}$ )  $^{99m}\text{Tc}$ -CGG- $\text{Z}_{\text{HER}2:342}$ . Six hours after injection of  $^{99m}\text{Tc}$ -CGG- $\text{Z}_{\text{HER}2:342}$ , the animals were killed by overdosing of Rompun/Ketalar. Imaging was performed using a Siemens gamma-camera equipped with a LEHR collimator at the Department of Nuclear Medicine of Uppsala University Hospital. Static images were collected during 10 min, and the images were evaluated with a Hermes system (Nuclear Diagnostic). A quantitative analysis was done by drawing equal regions of interest (ROI) over the tumor and contralateral thigh.

## RESULTS

**Peptide Synthesis.** The Fmoc solid-phase synthesis of  $\text{Z}_{\text{HER}2:342}$  resulted in a yield of 21% of the full-length peptide, as determined by analytical RP-HPLC. The  $^{99m}\text{Tc}$ -chelating sequences of CGG or CGGG introduced N-terminally by manual

**Table 3. Biodistribution of  $^{99m}\text{Tc}$ -CGG- $Z_{\text{HER2:342}}$  and  $^{125}\text{I}$ -PIB- $Z_{\text{HER2:342}}$  in Balb/c nu/nu Mice Bearing SKOV-3 Xenografts. Data Are Presented as % IA<sub>g</sub> (an Average From Four Animals  $\pm$  SEM)**

organ	1 h		4 h				6 h	
	$^{99m}\text{Tc}$	$^{125}\text{I}$	$^{99m}\text{Tc}$	$^{99m}\text{Tc}$ block	$^{125}\text{I}$	$^{125}\text{I}$ block	$^{99m}\text{Tc}$	$^{125}\text{I}$
blood	2.32 $\pm$ 0.44	3.75 $\pm$ 0.61	0.84 $\pm$ 0.20	1.07 $\pm$ 0.14	0.72 $\pm$ 0.20	0.52 $\pm$ 0.10	0.62 $\pm$ 0.08	0.25 $\pm$ 0.04
lung	1.80 $\pm$ 0.36	2.96 $\pm$ 0.47	0.69 $\pm$ 0.12	0.95 $\pm$ 0.14 <sup>c</sup>	0.71 $\pm$ 0.19	0.53 $\pm$ 0.14	0.50 $\pm$ 0.14	0.35 $\pm$ 0.14
liver	2.57 $\pm$ 0.46	5.38 $\pm$ 1.04	1.32 $\pm$ 0.16	1.33 $\pm$ 0.35	0.80 $\pm$ 0.13	0.68 $\pm$ 0.35	0.97 $\pm$ 0.09	0.27 $\pm$ 0.04
spleen	0.87 $\pm$ 0.16	2.06 $\pm$ 0.21	0.43 $\pm$ 0.19	0.58 $\pm$ 0.30	0.30 $\pm$ 0.06	0.33 $\pm$ 0.24	0.37 $\pm$ 0.15	0.12 $\pm$ 0.07
kidney	67.62 $\pm$ 12.85	34.76 $\pm$ 4.72	58.84 $\pm$ 8.76	53.96 $\pm$ 7.23	19.07 $\pm$ 4.70	11.83 $\pm$ 1.48	40.02 $\pm$ 4.00	7.75 $\pm$ 0.7
stomach	5.33 $\pm$ 1.00	2.45 $\pm$ 0.63	3.51 $\pm$ 0.39	5.44 $\pm$ 1.16 <sup>c</sup>	0.99 $\pm$ 0.40	0.61 $\pm$ 0.05	3.36 $\pm$ 0.70	0.41 $\pm$ 0.12
salivary gland	4.95 $\pm$ 1.20	2.65 $\pm$ 0.51	4.17 $\pm$ 0.73	6.15 $\pm$ 0.90 <sup>c</sup>	1.31 $\pm$ 0.23	0.91 $\pm$ 0.20 <sup>c</sup>	2.52 $\pm$ 0.74	0.40 $\pm$ 0.22
thyroid <sup>d</sup>	0.27 $\pm$ 0.08	0.19 $\pm$ 0.07	0.19 $\pm$ 0.04	0.33 $\pm$ 0.19	0.26 $\pm$ 0.09	0.25 $\pm$ 0.15	0.16 $\pm$ 0.01	0.34 $\pm$ 0.08
tumor	3.36 $\pm$ 0.78	3.51 $\pm$ 0.62	4.23 $\pm$ 1.03	1.26 $\pm$ 0.14 <sup>c</sup>	3.68 $\pm$ 0.98	0.84 $\pm$ 0.13 <sup>c</sup>	5.69 $\pm$ 2.29	5.38 $\pm$ 2.14
muscle	0.34 $\pm$ 0.08	0.53 $\pm$ 0.11	0.24 $\pm$ 0.05	0.26 $\pm$ 0.05	0.18 $\pm$ 0.04	0.13 $\pm$ 0.04	0.14 $\pm$ 0.04	0.04 $\pm$ 0.03
bone	0.98 $\pm$ 0.64	0.67 $\pm$ 0.30	0.36 $\pm$ 0.09	0.40 $\pm$ 0.19	0.16 $\pm$ 0.09	0.17 $\pm$ 0.13	0.45 $\pm$ 0.29	0.07 $\pm$ 0.06
intestine <sup>b</sup>	7.77 $\pm$ 1.62	6.19 $\pm$ 0.55	17.10 $\pm$ 0.83	17.27 $\pm$ 3.88	3.72 $\pm$ 0.44	2.63 $\pm$ 0.72	9.75 $\pm$ 3.11	2.03 $\pm$ 2.30

<sup>a</sup> Data for thyroid are presented as % IA per organ. <sup>b</sup> Data for intestine with content are presented as % IA per whole sample. <sup>c</sup> Statistically significant difference,  $p < 0.05$ .

synthesis, both resulting in total synthetic yields 16% (Table 1). After purification with RP-HPLC, the purity was higher than 90%. ESI-MS was used to verify the molecular weight of the peptides. For the MS analysis, the thiol groups were capped with iodoacetamide, resulting in an additional mass of 57 Da. The data obtained correlated well with the expected masses (Table 1).

**Biophysical Characterization.** The stability of the secondary structure of the different proteins was studied at variable temperatures. The melting temperatures of the CGG and CGGG-modified peptides were 68 °C (Table 1). The CD spectra were recorded before and after melting of each peptide, and all generated very similar spectra, showing  $\alpha$ -helical structure, suggesting that the proteins refold after heating to 90 °C.

**Biosensor Analysis.** The binding kinetics of the different Tc-chelating proteins were compared in a biospecific interaction analysis on a Biacore 2000 instrument. As shown in Table 1, both conjugates showed similar affinities to surface-immobilized HER2 receptors: 280 pM and 250 pM for CGG- $Z_{\text{HER2:342}}$  and CGGG- $Z_{\text{HER2:342}}$ , respectively.

**Radiolabeling.** As displayed in Table 2, the efficiency of the direct labeling of cysteine-containing Affibody molecules was much higher than for the indirect labeling method (>90% vs 54%). The isolated yield from size-exclusion chromatography using NAP-5 columns was about 70% from the direct labeling and about 50% from the indirect method. Typically, the radiochemical purity of conjugates after NAP-5 separation was over 98% for both labeling methods. The presence of reduced hydrolyzed technetium was less than 2% in all experiments (data not shown).

**Stability and Cell Binding of Labeled Conjugates.** The *in vitro* stability of the labeled conjugates was evaluated in PBS and cysteine. The incubation of the labeled Affibody molecules for 2 h in the presence of 300 molar excess of cysteine showed a reasonably high stability. Most of the radioactivity (approximately 70%) of  $^{99m}\text{Tc}$ -CGG- $Z_{\text{HER2:342}}$  and  $^{99m}\text{Tc}$ -CGGG- $Z_{\text{HER2:342}}$  was still attached to the labels. The stability in PBS was even higher, especially for  $^{99m}\text{Tc}$ -CGG- $Z_{\text{HER2:342}}$  with 90% attachment of technetium to the conjugate (Table 2).

The results of plasma stability test (Figure 2) showed that the conjugates were stable during 1 h at 37 °C. No release of radioactive low-molecular-weight products or association with serum proteins was observed. A small amount of radioactivity was associated with proteins bigger than the  $^{99m}\text{Tc}$ -CGG- $Z_{\text{HER2:342}}$  peak (Figure 2.A), which can indicate some transchelation to blood plasma proteins.

The binding specificity of  $^{99m}\text{Tc}$ -CGG- $Z_{\text{HER2:342}}$  and  $^{99m}\text{Tc}$ -CGGG- $Z_{\text{HER2:342}}$  was evaluated in the HER2-expressing ovarian cancer cell line SKOV-3. The binding was specific, since it

could be blocked with receptor saturation by 100-fold excess of unlabeled  $Z_{\text{HER2:342}}$  (data not shown). The antigen binding capacity was estimated to be around 60% for directly labeled  $^{99m}\text{Tc}$ -CGG- $Z_{\text{HER2:342}}$  and  $^{99m}\text{Tc}$ -CGGG- $Z_{\text{HER2:342}}$ . The difference in antigen binding capacity between directly and indirectly labeled  $^{99m}\text{Tc}$ -CGGG- $Z_{\text{HER2:342}}$  was not statistically significant. It should be noted that the testing method used in this study provides lower value in comparison with the Lindmo analysis but is much less laborious. We use it for comparison of conjugates, not to obtain a true value for binding to an infinite excess of antigen. The cellular retention for the conjugates is illustrated in Figure 3.  $^{99m}\text{Tc}$ -CGG- $Z_{\text{HER2:342}}$  and  $^{99m}\text{Tc}$ -CGGG- $Z_{\text{HER2:342}}$  displayed similar patterns at all time points. For comparison, the retention of a radioiodinated Affibody via a *p*-iodobenzoate linker,  $^{125}\text{I}$ -PIB- $Z_{\text{HER2:342}}$  (18), was also included, and it was found that the  $^{99m}\text{Tc}$ -labels exhibited higher retention than the radioiodinated conjugate ( $p < 0.001$ ), with about 50% cell-associated radioactivity 24 h after interrupted incubation, compared to 40% for iodine label.

**Comparative Biodistribution in Non-Tumor-Bearing NMRI Mice.** Figure 4 presents the biodistribution of the labeled conjugates in normal mice 4 h pi. For comparison, we also included the previously described  $^{99m}\text{Tc}$ -maGGG- $Z_{\text{HER2:342}}$  (22) in the study. The biodistribution studies showed rapid renal excretion with about 50% IA/g trapped in the kidneys for  $^{99m}\text{Tc}$ -CGG- and CGGG- $Z_{\text{HER2:342}}$  (both directly and indirectly labeled) 4 h pi, while the  $^{99m}\text{Tc}$ -maGGG- $Z_{\text{HER2:342}}$  displayed much lower uptake, less than 7% IA/g. In the previous study of  $^{99m}\text{Tc}$ -maGGG- $Z_{\text{HER2:342}}$  (22), we found that a high percentage of radioactivity was accumulated in the gastrointestinal tract, likely due to its excretion via the bile. In this study, we observed that the hepatobiliary excretion of the Affibody molecules was reduced with the use of CGG and CGGG chelators. The detected uptake in the intestines with their contents was about 12% IA/whole organ, an almost 3-fold reduction compared to when maGGG was used as chelator (32% IA/whole organ). Low levels of radioactivity were found in blood, lung, liver, stomach, salivary glands, spleen, and muscle for all conjugates.

The influence of injection route (intravenous or subcutaneous) on the biodistribution of  $^{99m}\text{Tc}$ -CGG- $Z_{\text{HER2:342}}$  was also evaluated. The comparison showed that biodistribution 4 h pi was similar in both cases (Figure 5), with a small but significant increase of radioactivity in liver, stomach, and salivary gland after subcutaneous injection. These results indicate a quick drainage of Affibody-based conjugates by lymphatic system.

**Tumor Targeting in Balb/c nu/nu Mice with SKOV-3 Xenografts.** The *in vivo* tumor-targeting properties of  $^{99m}\text{Tc}$ -CGG- $Z_{\text{HER2:342}}$  were evaluated through biodistribution studies on mice bearing HER2-expressing SKOV-3 xenografts, as

summarized in Table 3. In the same animals we also injected  $^{125}\text{I}$ -PIB- $Z_{\text{HER2:342}}$  to have a reference, as this conjugate had previously demonstrated good targeting properties (18). The results showed that the blood level of  $^{99\text{m}}\text{Tc}$ -CGG- $Z_{\text{HER2:342}}$  decreased rapidly, reaching  $2.32 \pm 0.44$  %IA/g 1 h pi and  $0.62 \pm 0.08$  %IA/g 6 h pi. The radioactivity clearance from other organs followed the same pattern. The tumor-to-kidney ratios were  $0.050 \pm 0.01$  (1 h pi),  $0.072 \pm 0.017$  (4 h pi), and  $0.147 \pm 0.074$  (6 h pi) for  $^{99\text{m}}\text{Tc}$ -CGG- $Z_{\text{HER2:342}}$ . The tumor uptake of  $^{99\text{m}}\text{Tc}$ -CGG- $Z_{\text{HER2:342}}$  did not differ significantly between the points of time.

To study the binding specificity to HER2-receptors *in vivo*, a group of mice were preinjected with a 1000-fold excess of nonlabeled Affibody molecule before injection of the labeled conjugates. As expected, the tumor uptake of both  $^{99\text{m}}\text{Tc}$ - and  $^{125}\text{I}$ -label in the blocked group was lower ( $p < 0.005$ ), which verified that the uptake was receptor-specific.

An Affibody molecule radioiodinated via a *p*-iodobenzoate linker,  $^{125}\text{I}$ -PIB- $Z_{\text{HER2:342}}$  (18), was used as an internal reference for comparison and was also injected into the same animals in this biodistribution study. As can be seen in Figure 6, the tumor-to-organ ratios were high for both  $^{99\text{m}}\text{Tc}$ -CGG- $Z_{\text{HER2:342}}$  and  $^{125}\text{I}$ -PIB- $Z_{\text{HER2:342}}$ . Generally, the technetium label provided better contrast 1 h pi. The uptake was approximately equal 4 h pi, but 6 h pi, the radioiodine label provided better tumor-to-organ ratios.

**Gamma-Camera Imaging of HER2-Expressing Xenografts Using  $^{99\text{m}}\text{Tc}$ -CGG- $Z_{\text{HER2:342}}$**  Gamma-camera images in BALB/c nu/nu mice bearing SKOV-3 tumors were acquired after 6 h after administration of  $^{99\text{m}}\text{Tc}$ -CGG- $Z_{\text{HER2:342}}$ . The images revealed good radioactivity accumulation in the tumors, which were clearly visualized, as shown in Figure 7. However, the uptake was high in the kidneys and in the abdomen area, which was predicted from the results of biodistribution study. Tumor-to-contralateral thigh was  $29 \pm 7$  (average  $\pm$  maximum error).

## DISCUSSION

Earlier studies demonstrated that the use of solid-phase peptide synthesis can provide monomeric forms of Affibody molecules, capable for binding to target proteins and site-specific attachment of chelators for  $^{111}\text{In}$  and  $^{99\text{m}}\text{Tc}$  (19, 22). However, the present peptide synthesis techniques would be inefficient in production of large multimeric Affibody molecules or fusion proteins. For recombinant production, which would be required in this case, an incorporation of synthetic chelators would be possible only as a separate process. A possible alternative has been proposed earlier for scFv (24–26), namely an incorporation of a terminal cysteine, which would form N3S chelator together with adjacent amino acids. Still, we had to take into account that direct translation of a labeling technique from one protein to another is not easy in the case of technetium, since the surrounding amino acids influence the stability of the chelate on one hand, and the chelator may affect the biodistribution properties of a targeting protein on the other (30, 31). It is well-known that a change of chelator has a dramatic influence on the pharmacokinetics of short peptides, such as somatostatin analogues (32, 33). It is also known that the biodistribution of antibodies and their fragments is relatively insensitive to the labeling method (34). But data concerning the biodistribution of intermediate size (5–10 kDa) molecules are rather scant.

The model Affibody molecule  $Z_{\text{HER2:342}}$  was synthesized for this study by a solid-phase peptide synthesis with N-terminal extensions of the CGG or CGGG sequences. The final products showed subnanomolar affinities for the HER2 receptor, suggesting no major negative effect of CGG or CGGG attachment on binding properties of  $Z_{\text{HER2:342}}$  (Table 1).

Initial experiments on labeling of CGGG- $Z_{\text{HER2:342}}$  with  $^{99\text{m}}\text{Tc}$  were performed using tartrate as an intermediate weak

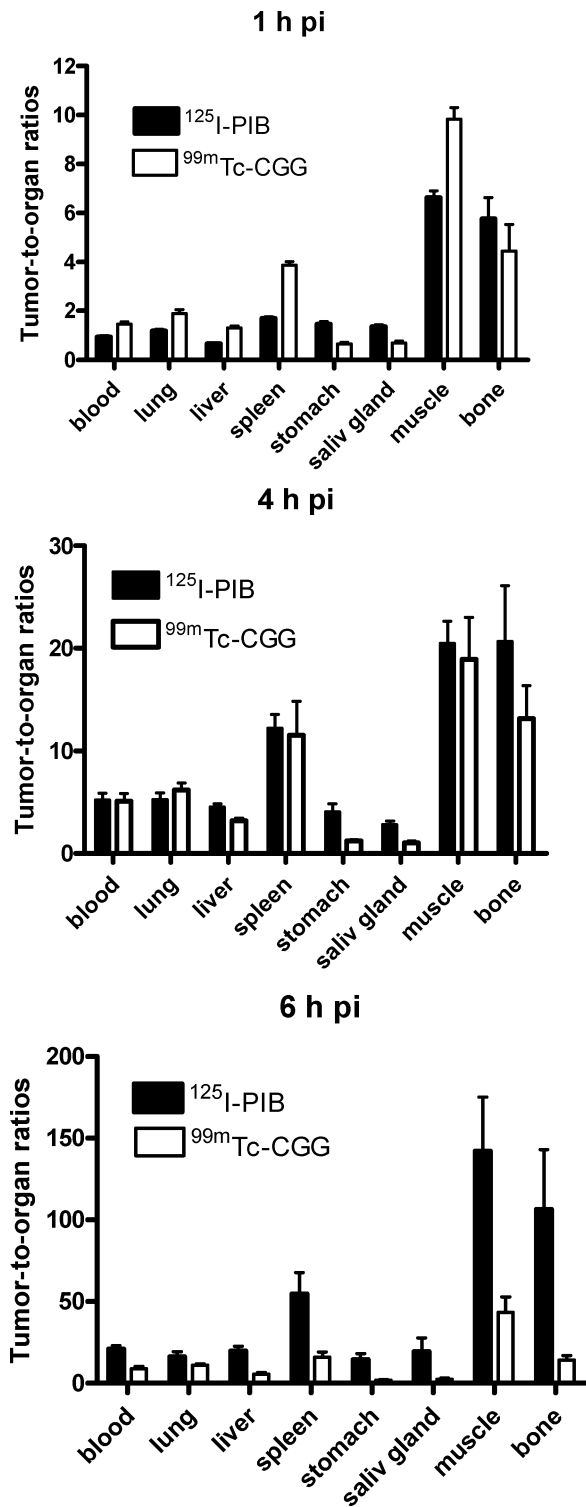


**Figure 6.** Tumor-to-organ ratios for  $^{99\text{m}}\text{Tc}$ -CGG- $Z_{\text{HER2:342}}$  and  $^{125}\text{I}$ -PIB- $Z_{\text{HER2:342}}$  in Balb/c nu/nu mice bearing SKOV3 xenografts. Data are presented as average from four animals  $\pm$  SEM.

chelator, i.e., by an indirect method. The labeling efficiency (Table 2) was  $53.8 \pm 10.1\%$ , which is lower than obtained for maGGG-containing  $Z_{\text{HER2:342}}$  conjugate (about 80%) (22). George and co-workers (24) have reported that labeling of scFv containing the GGGC sequence provided higher labeling yields (about 97%) in an alkaline condition. Alkaline pH is usually favorable for rapid  $^{99\text{m}}\text{Tc}$ -labeling, probably because of deprotonation of sulfur and nitrogen donor atoms, which facilitates the complexation of technetium (35, 36). The direct labeling method in alkaline solution (0.15 M NaOH, pH  $\sim$  11) provided a high radiochemical yield (90%), and a stable technetium

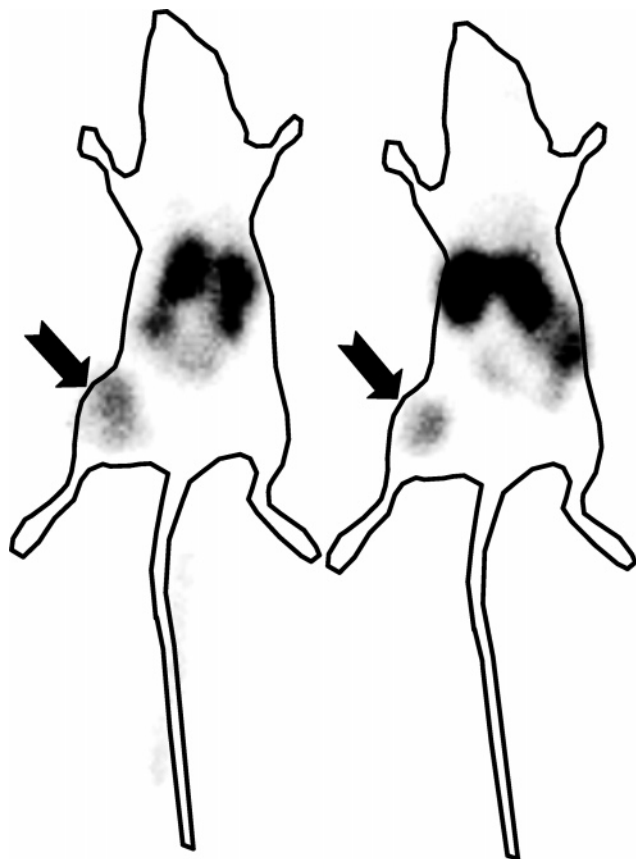


**Figure 7.** Gamma camera imaging of  $^{99m}\text{Tc}$ -CGG- $Z_{\text{HER2}:342}$  in Balb/c nu/nu mice bearing SKOV3 xenografts after 6 h pi.

labeling was achieved. The specificity of binding to HER2 *in vitro* after direct labeling was preserved, and the antigen binding capacity did not differ significantly from the capacity after indirect labeling. No significant difference in biodistribution was found between directly and indirectly labeled CGGG- $Z_{\text{HER2}:342}$  (Figure 4). For this reason, direct labeling was selected for CGG- $Z_{\text{HER2}:342}$  labeling as well. The plasma stability in mouse serum indicated that the labeled conjugates were stable during 1 h. It was found that the retention of radioactivity in malignant SKOV-3 cells was better for  $^{99m}\text{Tc}$ -labeled cysteine-containing conjugates than for a radioiodinated counterpart (Figure 3). This can be explained by better intracellular retention of radiocatabolites after internalization and lysosomal degradation of Affibody molecules.

The primary purpose of the development of an imaging agent lies in achieving high tumor-to-organ ratios, giving high contrast images. Therefore, a quick clearance from blood and unspecific compartments and quick tumor localization are essential properties of a targeting conjugate. Comparative biodistribution in normal mice (Figure 4) showed that the labeled conjugates had rather rapid blood clearance, with less than 1% IA/g at 4 h pi. This is in the same range (0.3–1.8% IA/g) as in mice for  $^{99m}\text{Tc}$ -labeled somatostatin analogues (37) and lower than the blood level reported at that time for  $^{99m}\text{Tc}$ -labeled scFv (38) or their multimeric constructs (39). The low blood radioactivity concentration suggested that, in agreement with the *in vitro* serum stability test, no considerable transchelation to blood plasma proteins occurred. Low levels of radioactivity were detected in liver and lungs, suggesting that no colloids were formed. However, a somewhat elevated radioactivity (in comparison with  $^{99m}\text{Tc}$ -maGGG- $Z_{\text{HER2}:342}$ ) in stomach and salivary glands was observed, indicating some release of free pertechnetate. Since the conjugates appeared to be stable in blood plasma, it is likely that the release occurred during the

catabolism of the labeled conjugates in kidney, probably due to reoxidation. Furthermore, the  $^{99m}\text{Tc}$ -labeled cysteine-based chelators behaved similarly, while the most essential difference between these chelators and the maGGG chelator could be seen in the radioactivity accumulation in intestines. The results showed a 3-fold reduction of hepatobiliary excretion in the case of cysteine-based chelators in comparison with maGGG- $Z_{\text{HER2}:342}$ . An explanation of this effect could be that the use of cysteine instead of mercaptoacetyl as a thiol group donor increases the overall hydrophilicity of the chelate due to the presence of a charged amino group and shifts excretion pathway from hepatobiliary to renal. A number of studies indicate that the use of more hydrophilic  $^{99m}\text{Tc}$  chelates favor renal excretion (31, 37, 40, 41). A shift to renal excretion was also indicated in this study by the increase of the kidney uptake of a factor of 7 by exchanging the maGGG chelator to cysteine-based chelators. It might be surprising that an additional charged group caused such profound difference in biodistribution of a 7-kDa protein. However, similar effects were also reported by Zhu and co-workers (41) for a neutrophil elastase inhibitor HNE2, which is similar in size (about 7 kDa) to the Affibody molecules. In that study, a variation of a single amino acid (phenylalanine, glycine, or glutamic acid) in the chelator modified the biodistribution of the protein in the same way as in our experiments.

The *in vitro* results showed that both  $^{99m}\text{Tc}$ -CGG- $Z_{\text{HER2}:342}$  and  $^{99m}\text{Tc}$ -CGGG- $Z_{\text{HER2}:342}$  provided promising characteristics as targeting agents for HER2. To further evaluate the targeting properties, one of the conjugates ( $^{99m}\text{Tc}$ -CGG- $Z_{\text{HER2}:342}$ ) was investigated in nude mice carrying SKOV-3 xenografts. Biodistribution data from the blocking experiment of  $^{99m}\text{Tc}$ -CGG- $Z_{\text{HER2}:342}$  demonstrated that the binding to HER2 receptors in ovarian carcinoma tumors was receptor-specific, since the uptake was blocked by a preinjection of an excess of nonlabeled Affibody ( $p < 0.005$ ). The *in vivo* retention in tumors was constant over time, which corresponded well with the results of the *in vitro* cellular retention study in SKOV-3 cells. Moreover,  $^{99m}\text{Tc}$ -CGG- $Z_{\text{HER2}:342}$  had a fast blood clearance and low uptake in most organs and was mainly excreted through kidneys, thus providing a low background for imaging. At early time points (1 and 4 h pi), the technetium label provided tumor-to-organ ratios that were similar to or better than those provided by  $Z_{\text{HER2}:342}$  radioiodinated using *p*-iodobenzoate. At 6 h pi, the radioiodine label was superior, probably due to a different pattern of clearance of radiocatabolites. However, the contrast level provided by the technetium label (e.g., tumor-to-blood ratio of 9.2) is acceptable. For clinical use, the  $^{99m}\text{Tc}$ -labeled conjugate might be preferred over the  $^{125}\text{I}$ -labeled one, due to the easy labeling (with a potential for a kit formulation), better logistics, and much lower price. Only a clinical study can answer if these factors may outweigh the somewhat lower contrast in comparison with the radioiodinated counterpart.

Gamma-camera imaging with  $^{99m}\text{Tc}$ -CGG- $Z_{\text{HER2}:342}$  at 6 h pi clearly showed the tumors in the mice. Although the accumulation in the intestines was largely reduced in comparison with the use of maGGG-chelator, the amount of radioactivity (10% IA per whole content) could still complicate the detection of extrahepatic metastases in the abdominal area on the day of injection. Nevertheless, the Affibody molecules seem to exhibit as good tumor-to-organ ratios as the other technetium-labeled anti-HER2 conjugates, if not better. For instance,  $^{99m}\text{Tc}$ -HYNIC-trastuzumab Fab (42) and  $^{99m}\text{Tc}$ -scFv barnase barstar constructs (43) had tumor-to-blood-ratios of 1.3 at 6 h pi and 10.8 at 24 h pi, respectively, compared to 9.2 at 6 h pi for the  $^{99m}\text{Tc}$ -labeled Affibody molecule. This comparison would give some ideas about the *in vivo* properties but should be interpreted with care, as different HER2-xenografts and sampling techniques were used.

In summary, the Affibody molecules containing cysteine-based chelators CGG and CGGG were stably labeled with  $^{99m}\text{Tc}$ , rapidly cleared from the blood circulation, and provided specific tumor accumulation (the latter case was for  $^{99m}\text{Tc}$ -CGG- $Z_{\text{HER2}:342}$ ). It was evident that  $^{99m}\text{Tc}$ -CGG- $Z_{\text{HER2}:342}$  clearly showed tumors in mice in the gamma-camera study. Thus, incorporation of cysteine into recombinant Affibody molecules would provide an efficient way for site-specific labeling of these proteins.

#### ACKNOWLEDGMENT

The authors thank Dr. Lars Abrahmsén, Dr. Joachim Feldwisch, and Dr. Anders Wennborg from Affibody AB for intellectual discussions. Thanks to Mrs. Aseel Cherif for providing us with Tc-generator eluate, Mrs. Veronika Eriksson for keeping the cell lab in excellent working conditions, and the staff of the animal department at Rudbeck laboratory. We thank Gustav Sundqvist at KTH for running the ESI-MS analyses. Financial support was provided by the Swedish Cancer Society (Cancerfonden) and the Swedish Research Council (Vetenskapsrådet).

#### LITERATURE CITED

- Baselga, J. (2006) Targeting tyrosine kinases in cancer: the second wave. *Science* 312, 1175–1178.
- Zidan, J., Dashkovsky, I., Stayerman, C., Basher, W., Cozacov, C., and Hadary, A. (2005) Comparison of HER-2 overexpression in primary breast cancer and metastatic sites and its effect on biological targeting therapy of metastatic disease. *Br. J. Cancer*. 93, 552–556.
- Heppeler, A., Froidevaux, S., Eberle, A. N., and Maেকে, H. R. (2000) Receptor targeting for tumor localisation and therapy with radiopeptides. *Curr. Med. Chem.* 94, 971–994.
- Mosesson, Y., and Yarden, Y. (2004) Oncogenic growth factor receptors: implications for signal transduction therapy. *Semin. Cancer Biol.* 14, 262–270.
- Jain, R. K. (1987) Transport of molecules across tumor vasculature. *Cancer Metastasis Rev.* 6, 559–593.
- Smith-Jones, P. M., Solit, D. B., Akhurst, T., Afroze, F., Rosen, N., and Larson, S. M. (2004) Imaging the pharmacodynamics of HER2 degradation in response to Hsp90 inhibitors. *Nat. Biotechnol.* 22, 701–706.
- Weiner, M. L. and Adams, G. P. (2000) New approaches to antibody therapy. *Oncogene* 19, 6144–6151.
- Van, de Wiele, C., Revets, H., and Mertens, N. (2004) Radioimmunoimaging. Advances and prospects. *Q. J. Nucl. Med. Mol. Imaging* 48, 317–325.
- Nord, K., Gunneriusson, E., Ringdahl, J., Stahl, S., Uhlen, M., and Nygren, P.-A. (1997) Binding proteins selected from combinatorial libraries of an alpha-helical bacterial receptor domain. *Nat. Biotechnol.* 15, 772–777.
- Wikman, M., Steffen, A.-C., Gunneriusson, E., Tolmachev, V., Adams, G. P., Carlsson, J., and Stahl, S. (2004) Selection and characterisation of HER2/neu-binding affibody ligands. *Protein Eng. Des. Sel.* 17, 455–462.
- Stern, D. F., Heffernan, P. A., and Weinberg, R. A. (1986) p185, a product of the neu proto-oncogene, is a receptorlike protein associated with tyrosine kinase activity. *Mol. Cell. Biol.* 6, 1729–1740.
- Slamon, D. J., Clark, G. M., Wong, S. G., Levin, W. J., Ullrich, A., and McGuire, W. L. (1987) Human breast cancer: correlation of relapse and survival with amplification of the HER-2/neu oncogene. *Science* 235, 177–182.
- Bast, R. C., Jr., Ravdin, P., Hayes, D. F., Bates, S., Fritsche, H., Jessup, J. M., Kemeny, N., Locker, G. Y., Mennel, R. G., and Somerfield, M. R. American Society of Clinical Oncology Tumor Markers Expert Panel. (2001) 2000 update of recommendations for the use of tumor markers in breast and colorectal cancer: clinical practice guidelines of the American Society of Clinical Oncology. *J. Clin. Oncol.* 19, 1865–1878.
- Molina, R., Barak, V., van Dalen, A., Duffy, M. J., Einarsson, R., Gion, M., Goike, H., Lamerz, R., Nap, M., Sölétormos, G., and Stieber, P. (2005) Tumor markers in breast cancer- European Group on Tumor Markers recommendations. *Tumor Biol.* 26, 281–293.
- Steffen, A.-C., Orlova, A., Wikman, M., Gunneriusson, E., Nilsson, F. Y., Adams, G. P., Tolmachev, V., and Carlsson, J. (2006) Affibody mediated tumor targeting of HER-2 expressing xenografts in mice. *Eur. J. Nucl. Med. Mol. Imaging* 33, 631–638.
- Orlova, A., Nilsson, F. Y., Wikman, M., Ståhl, S., Carlsson, J., and Tolmachev, V. (2006) Comparative in vivo evaluation of iodine and technetium labels on anti-HER2 affibody for single-photon imaging of HER2 expression in tumors. *J. Nucl. Med.* 47, 512–519.
- Mume, E., Orlova, A., Nilsson, F. Y., Larsson, B., Nilsson, A. S., Sjöberg, S., and Tolmachev, V. (2005) Evaluation of ((4-hydroxyphenyl)ethyl)maleimide for site-specific radiobromination of anti-HER2 affibody. *Bioconjugate Chem.* 16, 1547–1555.
- Orlova, A., Magnusson, M., Eriksson, T., Nilsson, M., Larsson, B., Höiden-Guthenberg, I., Widstrom, C., Carlsson, J., Tolmachev, V., Stahl, S., and Nilsson, F. Y. (2006) Tumor imaging using a picomolar affinity HER-2 binding affibody molecules. *Cancer Res.* 66, 4339–4348.
- Tolmachev, V., Nilsson, F. Y., Widstrom, C., Andersson, K., Rosik, D., Gedda, L., Wennborg, A., and Orlova, A. (2006)  $^{111}\text{In}$ -benzyl-DTPA- $Z_{\text{HER2}:342}$ , an Affibody-based conjugate for *in vivo* imaging of HER2 expression in malignant tumors. *J. Nucl. Med.* 47, 846–853.
- Orlova, A., Tolmachev, V., Pehrson, R., Lindborg, M., Tran, T., Sandström, M., Nilsson, F.Y., Wennborg, A., Abrahmsén, L., and Feldwisch, J. (2007) Synthetic Affibody molecules: A novel class of affinity ligands for molecular imaging of HER2 expressing malignant tumors. *Cancer Res.*, in press.
- Baum, R. P., Orlova, A., Tolmachev, V., and Feldwisch, J. (2006) Receptor PET/CT and SPECT using an Affibody molecule for targeting and molecular imaging of HER2 positive cancer in animal xenografts and human breast cancer patients. *J. Nucl. Med.* 47, 108.
- Engfeldt, T., Orlova, A., Tran, T., Bruskin, A., Widstrom, C., Eriksson Karlstrom, A., and Tolmachev, V. (2006) Imaging of HER2-expressing tumors using a synthetic affibody containing  $^{99m}\text{Tc}$ -chelating mercaptoacetyl-GGG sequence. *Eur. J. Nucl. Med. Mol. Imaging*, [Epub ahead of print] PMID 17146656.
- Tolmachev, V., Orlova, A., Pehrson, R., Galli, J., Baastrup, B., Andersson, K., Sandström, M., Rosik, D., Carlsson, J., Lundqvist, H., Wennborg, A., and Nilsson, F. Y. (2007) Radionuclide therapy of HER2-positive microxenografts using a  $^{177}\text{Lu}$ -labeled HER2-specific Affibody molecule. *Cancer Res.* 67 (6).
- George, A. J., Jamar, F., Tai, M. S., Heelan, B. T., Adams, G. P., McCartney, J. E., Houston, L. L., Weiner, L. M., Opperman, H., and Peters, A. M. (1995) Radiometal labeling of recombinant proteins by a genetically engineered minimal chelation site: Technetium-99m coordination by single-chain Fv antibody fusion proteins through a C-terminal cysteinyl peptide. *Proc. Natl. Acad. Sci. U.S.A.* 92, 8358–8362.
- Tolbert, T. J., and Wong, C. H. (2002) New methods for proteomic research: Preparation of proteins with N-terminal cysteines for labeling and conjugation. *Angew. Chem., Int. Ed.* 41, 2111–2174.
- Liberatore, M., Neri, D., Neri, G., Pini, A., Iurilli, A. P., Ponzio, F., Spampinato, G., Padula, F., Pala, A., and Colella, A. C. (1995) Efficient one-step direct labelling of recombinant antibodies with technetium-99m. *Eur. J. Nucl. Med.* 22, 1326–1329.
- Verhaar, M. J., Keep, P. A., Hawkins, R. E., Robson, L., Casey, J. L., Pedley, B., Boden, J. A., Begent, R. H., and Chester, K. A. (1996) Technetium-99m radiolabeling using a phage-derived single-chain Fv with a C-terminal cysteine. *J. Nucl. Med.* 37, 868–872.
- Engfeldt, T., Renberg, B., Brumer, H., Nygren, P.-A., and Eriksson Karlstrom, A. (2005) Chemical synthesis of triple-labeled three-helix bundle binding proteins for specific fluorescent detection of unlabeled protein. *ChemBioChem* 6, 1043–1050.
- Winnard, P. Jr., Chang, F., Rusckowski, M., Mardirosian, G., and Hnatowich, D. J. (1997) Preparation and use of NHS-MAG3 for technetium-99m labeling of DNA. *Nucl. Med. Biol.* 24, 425–432.

- (30) Vanderheyden, J. L., Liu, G., He, J., Patel, B., Tait, J. F., and Hnatowich, D. J. (2006) Evaluation of  $^{99m}\text{Tc}$ -MAG3-annexin V: influence of the chelate on *in vitro* and *in vivo* properties in mice. *Nucl. Med. Biol.* 33, 135–144.
- (31) Qu, T., Wang, Y., Zhu, Z., Rusckowski, M., and Hnatowich, D. J. (2001) Different chelators and different peptides together influence the *in vitro* and mouse *in vivo* properties of  $^{99m}\text{Tc}$ . *Nucl. Med. Commun.* 22, 203–215.
- (32) Froidevaux, S., Heppeler, A., Eberle, A. N., Meier, A. M., Hausler, M., Beglinger, C., Behe, M., Powell, P., and Macke, H. R. (2000) Preclinical comparison in AR4–2. J tumor-bearing mice of four radiolabeled 1,4,7,10-tetraazacyclododecane-1,4,7,10-tetraacetic acid-somatostatin analogs for tumor diagnosis and internal radiotherapy. *Endocrinology* 141, 3304–3312.
- (33) Eisenwiener, K. P., Prata, M. I., Buschmann, I., Zhang, H. W., Santos, A. C., Wenger, S., Reubi, J. C., and Macke, H. R. (2002) NODAGATOC, a new chelator-coupled somatostatin analogue labeled with [ $^{67/68}\text{Ga}$ ] and [ $^{111}\text{In}$ ] for SPECT, PET, and targeted therapeutic applications of somatostatin receptor (hsst2) expressing tumors. *Bioconjugate Chem.* 13, 530–541.
- (34) Liu, S. and Edwards, D. S. (1999)  $^{99m}\text{Tc}$ -labeled small peptides as diagnostic radiopharmaceuticals. *Chem. Rev.* 9, 2235–2268.
- (35) Bormans, G., Cleynhens, B., Adriaens, P., Vanbilloen, H., De Roo, M., and Verbruggen, A. (1995) Investigation of the labeling characteristics of  $^{99m}\text{Tc}$ -mercaptoacetyltryglycine. *Nucl. Med. Biol.* 22, 339–349.
- (36) Thakur, M. L., Pallela, V. R., Consigny, P. M., Rao, P. S., Vessileva-Belnikolovska, D., and Shi, R. (2000) Imaging vascular thrombosis with  $^{99m}\text{Tc}$ -labeled fibrin alpha-chain peptide. *J. Nucl. Med.* 41, 161–168.
- (37) Decristoforo, C., and Mather, J. S. (1999) Technetium-99m somatostatin analogues: effect of labeling methods and peptide sequence. *Eur. J. Nucl. Med.* 26, 869–876.
- (38) Pietersz, G. A., Patrick, M. R., and Chester, K. A. (1998) Preclinical characterization and *in vivo* imaging studies of an engineered recombinant technetium-99m-labeled metallothionein-containing anti-carcinoembryonic antigen single-chain antibody. *J. Nucl. Med.* 39, 47–56.
- (39) Goel, A., Baranowska-Kortylewicz, J., Hinrichs, S. H., Wisecarver, J., Pavlinkova, G., Augustine, S., Colcher, D., Booth, B. J., and Batra, S. K. (2001)  $^{99m}\text{Tc}$ -labeled divalent and tetravalent CC49 single-chain Fv's: novel imaging agents for rapid *in vivo* localization of human colon carcinoma. *J. Nucl. Med.* 42, 1519–1527.
- (40) Verbeke, K., Snauwaert, K., Cleynhens, B., Scheer, W., and Verbruggen, A. (2000) Influence of the bifunctional chelate on the biological behavior of  $^{99m}\text{Tc}$ -labeled chemotactic peptide conjugates. *Nucl. Med. Biol.* 27, 769–779.
- (41) Zhu, Z., Wang, Y., Zhang, Y., Liu, G., Liu, N., Rusckowski, M., and Hnatowich, D. J. (2001) A novel and simplified route to the synthesis of N3S chelators for  $^{99m}\text{Tc}$  labeling. *Nucl. Med. Biol.* 28, 703–708.
- (42) Tang, Y., Scollard, D., Chen, P., Wang, J., Holloway, C., and Reilly, M. R. (2005) Imaging of HER2/neu expression in BT-373 human breast cancer xenografts in athymic mice using ( $^{99m}\text{Tc}$ )-HYNIC-trastuzumab (Herceptin) Fab fragments. *Nucl. Med. Commun.* 26, 427–432.
- (43) Deyev, S. M., Waibel, R., Lebedenko, E. N., Schubiger, A. P., and Plückthun, A. (2003) Design of multivalent complexes using barnase\*barstar module. *Nat. Biotechnol.* 21, 1486–1492.

BC060291M